ASEAN Journal of Chemical Engineering 2023, Vol. 23, No. 2, 224 – 239

Enhancing the Anti-Fouling Property of Polyethersulfone-based Membrane using Chitosan Additive from Golden Snail *(Pomacea canaliculata)* Shell Waste for Water Purification

Sri Mulyati [*,1]
Cut Meurah Rosnelly [1]
Yanna Syamsuddin [1]
Nasrul Arahman [1]
Syawaliah Muchtar [1]
Wahyuni [1]
Tiara Lauzia [1]
Aulia Chintia Ambarita [2]
Muhammad Roil Bilad [3]
Shafirah Samsuri [4]
[1] *Department of Chemical Engineering, Universitas Syiah Kuala, Banda Aceh 23111, Indonesia*
[2] *Doctoral Program, School of Engineering Science, Syiah Kuala University, Banda Aceh 23111, Indonesia*
[3]*Faculty of Integrated Technologies, Universiti Brunei Darussalam, Jalan Tungku Link, Gadong, BE 1410, Brunei*
[4]*Chemical Engineering Department, Universiti Teknologi PETRONAS, Seri Iskandar 32610, Perak, Malaysia*
[*]e-mail: sri.mulyati@usk.ac.id

Submitted 6 January 2023 *Revised* 28 February 2023 *Accepted* 5 April 2023

Abstract. One of the common techniques for treating water and water from waste effluent is membrane filtration. Polymer is the main material that is most extensively employed as a substance for membranes. Because of its outstanding strength and resistance to chemicals, Polyethersulfone, also known as PES, is a common polymer used in the production of membranes. Unfortunately, its hydrophobicity makes it easy to foul when applied to water treatment processes. This study introduced a chitosan additive isolated from golden snail shell waste as an additive for PES-based membrane fabrication via blending at 0 wt%, 1 wt%, 3 wt%, 5 wt%, and 7 wt%. After preparation, the resultant membranes were analyzed and tested for their ability to filter a humic acid solution at a concentration of 50 mg L^{-1}. According to the findings, the chitosan additive has the potential to change the characteristics of the membrane as well as its filtration performance. It increased the pure water flux from 110 181 L m^{-2} h^{-1} (no chitosan loading) to 181 L m^{-2} h^{-1} (for five wt% loadings). The membrane characterization results supported this increase in pure water flux, which showed that adding chitosan additives improved the porosity, size of pores, and hydrophilicity. The addition of this additive also has a good effect on the anti-fouling property by increasing the fouling recovery ratio (FRR). The FRRs for the modified membranes were 79% to 82%, which were higher than the neat PES membrane with an FRR of merely 60%.

Keywords: Chitosan, Humic Acid, Membrane Fouling, *Pomacea canaliculata*, Water Filtration

DOI: 10.22146/ajche.79643

INTRODUCTION

Conventionally, water treatment can be carried out by coagulation, sedimentation, filtration, disinfection, decontamination, desalination, etc. (Ali, 2012). One process that has attracted recent attention is membrane filtration. Because of its high performance, low energy consumption, excellent selectivity, absence of phase change, and ability to be operated at room temperature, it has found widespread application in a variety of industries, including the food and beverage industry, the pharmaceutical industry, biotechnology, and the water treatment industry, amongst others (Liu et al. 2017). In addition, this technology also has the advantage that the membrane can be applied in a small space and uses fewer chemicals (Vatsha et al. 2014). Besides the advantages of this technology, this technology also has a drawback, which is the high fouling propensity on the surface of the membrane. Because of the presence of these impurities, the implementation of membrane technology may be restricted. Membrane fouling is the result of the deposition or preservation of a wide variety of substances on the surface of the membrane or in the holes of the membrane. Membrane fouling can cause a reduction in the membrane's ability to function properly and can even lead to the failure of the membrane entirely. There are many kinds of membrane fouling, including those that are caused by inorganic substances (Miller et al. 2014), organic compounds (Rambabu et al. 2019), colloids, and biofouling (Wang et al. 2022). Membrane fouling causes a decrease in permeability, resulting in increased operating costs and more energy for filtration (Vatsha et al. 2014).

There are several factors that affect the separation performance of an ultrafiltration process, including the properties of the employed membrane material. Polymer-based membranes are one of the most popular in their use. One of them is polyethersulfone (PES) membrane. It is due to the advantages of PES membranes which have good chemical resistance and thermal and mechanical stability and have been widely used for industrial applications. However, poor hydrophilic properties limit the performance and application of PES membranes (Rambabu et al. 2019). However, the hydrophobic properties of this PES polymer encourage the attachment and build-up of pollutants on the surface of the membrane during filtration, clogging the membrane pores and causing membrane fouling and flux decrease (Wang et al. 2022). Pollutants such as humic acid, protein, or surfactants are naturally present in the water. These contaminants are hydrophobic, which means that they associate favorably with the membrane surface that also possesses these characteristics (Yuan et al. 2018, Gao et al. 2019, Zhu et al. 2018, Guan et al. 2018).

One of the most dangerous naturally occurring organic pollutants in water systems is humic acid, which is produced by the microbiological decay of plants and animals (Ouda et al. 2022). Its presence in water can cause membrane fouling. To enhance the performance of membranes, several research have looked into the possibility of adding both organic and inorganic additives. These additives include low-weight PEG, which provides good performance for the separation of dyes and salts (Idris et al. 2007), CuO and ZnO (Nasrollahi et al. 2018), silica (Shen et al. 2011), and dopamine (Muchtar et al. 2019) .

Chitosan can also be used as an additive to increase membrane's hydrophilic nature (Chrzanowska et al. 2018, Zhao et al. 2021).

Chitosan is a polysaccharide compound composed of D-glucosamine and N-acetyl-D-glucosamine that is produced through the deacetylation of chitin. Chitosan has non-toxic, anti-bacterial, hydrophilic, biodegradable, good biocompatibility, low cost, and renewable properties. Chitosan has the ability to enhance the mechanical properties of polymers, however, because it contains amino and hydroxyl groups, it is also capable of performing the function of an adsorbent (Ghaemi et al. 2018). Chitosan is considered a superior adsorbent especially attributed to its dynamic swelling properties and functional groups (Rahmi et al. 2022).

Chitosan formed from chitin can be obtained from the shell of Golden Snail (*Pomacea canaliculata*), which becomes a pest of rice fields and is often used as animal feed. So far, Golden Snail shells still have minimum economic value but have been explored for various applications. Processing golden snail shells into chitosan can in-crease its economic value and promote the circular economy. A few reports on the utilization of Golden Snails' shells included for catalyst, adsorbent and liming materials (Phewphong et al. 2022, Jubaedah et al. 2018, Hariani et al. 2020). To the best of the writers' knowledge, using chitosan from golden snail shells as an additive in the manufacture of PES membranes has never been done before. However, the incorporation of chitosan extracted from the shell of the golden snail is expected to increase the overall properties (chemical and physical) enhancing the filtration efficiency of the resulting membrane just like chitosan derived from other established sources. Earlier reports demonstrated the effectiveness of chitosan and its derivative as a membrane fabrication additive in enhancing the resulting membrane anti-fouling properties (Nayab et al. 2021, Susanto et al. 2020, Elizalde et al. 2018, Kumar et al. 2013). In addition, utilizing golden snails is an option for reducing the accumulation of golden snail shells, which are abundant as a nuisance in agriculture activities.

The purpose of this research was to create a membrane made of PES by incorporating a chitosan additive that was obtained from waste. The attributes of chitosan were expected to improve the final membrane characteristics and performance against fouling. The synthesis of chitosan from golden snail shell waste was first carried out, then was used as additive to prepare PES-based membranes. The phase inversion method was used to synthesize the membrane. The prepared chitosan was blended with the primary PES polymer in the dope solution. The membranes were then characterized and evaluated for humic acid solution filtration as it is the most prevalent and predominant form of contaminant in groundwater.

MATERIALS AND METHODS

Materials

Shell waste of golden snail was obtained from rice farm in Aceh Besar, Indonesia. Polyethersulfone (PES, Ultrason E6020 P, BASF, Germany) was used as the main polymer for membrane fabrication. N-Methyl-2-pyrrolidone (NMP) was used as the solvent. NaOH (Merck, ACS reagent, ≥99.0%) was used for deproteination of the shell, deacetylation of chitin and resulting membrane stability under alkali condition. HCl (Merck, 37%) was used for demineralization process. Distilled water was used as the nonsolvent of the PES during the phase inversion process, the feed for pure water permeability (PWP) analysis and as the

solvent in humic acid solution. Humic acid was used as a model foulant of surface water feed during the filtration test.

Preparation of Chitosan from The Shell of Golden Snail

The protocol for chitosan preparation from the shell of golden snail is presented in Fig. 1. The golden snail's shells were washed and boiled for 15 min. Then, they were crushed and sieved to form powder with size of <200 mesh. The first stage was the demineralizing process where 100 gram of shell powder was introduced into HCl 1 N at a ratio of 1:7 (wt/v) then stirred at 200 rpm, heated to 80-90 °C for 1 h. The following step in the deproteination procedure involved adding 3.5 v% of NaOH at a ratio of 1:10 (wt/v), followed by heating the mixture at 70-80 °C for one hour. Subsequently, in the acetalization process, it was dissolved using 50% NaOH solution at a ratio of 1:15 (wt/v), heated at 80-90 °C while stirred at 200 rpm for 2 h. The resulting powder was then filtered, washed, and dried in an oven at 100 °C. The resulting powder was weighed repeatedly until it reached a consistent value. The chitosan powder was characterized using FTIR (Fourier Transformed Infrared Spectroscopy).

Membrane Preparation

In this work, five PES membranes were prepared with composition formulas as shown in Table 1. The polymer solution was made by diluting 15 wt% PES into the NMP solvent. The chitosan additive was loaded at 0 wt% (reference), 1 wt%, 3 wt%, 5 wt% , and 7 wt%, introduced into the PES solution. After stirring, the resulting homogeneous solution was poured onto a glass plate and cast into a thin sheet using a casting knife with a wet thickness of 300 micrometers. Subsequently, the film was put through an immersion precipitation process by placing it in a coagulation tank that contained distilled water. This made the process possible. The solidified film was let under water until it delaminated from the glass plate.

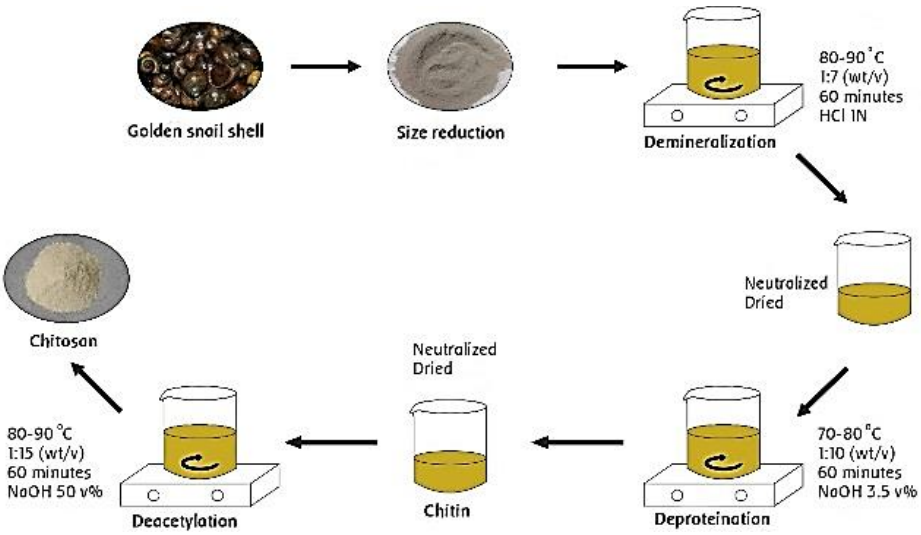

Fig. 1: The schematic representation of chitosan preparation from golden snail shells

Table 1. Composition of the casting solution

Membrane	PES (%w)	Chitosan (%w)	NMP (%w)
M1	15	0	85
M2	15	1	84
M3	15	3	82
M4	15	5	80
M5	15	7	78

Membrane Characterization

Surface Hydrophilicity Property

Water contact angle (WCA) measurements were made on the desiccated membrane surface to gauge the hydrophilicity of its surface. On the surface of the membrane, one microliter of Milli-Q water was deposited, and the contact angles were determined with the help of a goniometer (Attension, Terralab Laboratuvar Malzemeleri San. Tic. A.Ş.). A sample of the membrane was transferred to a glass plate with the assistance of double-sided tapes. Using a micro-syringe pipet, the distilled water was gently poured onto the surface of the membrane. Ten different measurements were taken of each membrane, the average and standard deviation of those measurements were taken for presentation.

Morphology Analysis

With a 20 kV voltage Field-Emission SEM (SEM, JEOL JSM-6360 LA), the membrane surface structure was examined. The material was dried in a freeze-dryer (FD-1000, Eyela, Japan) prior to analysis. An osmium coating was applied to the sample using an osmium coater (Neoc-STB, Meiwafosis Co. Ltd., Japan), promoting the conductivity needed to produce high-quality SEM images.

Surface Chemistry Analysis

The Fourier Transform Infrared (PerkinElmer spectrum 100 FT-IR.) analysis was done to identify the chemical bonds and functional groups presented on the prepared membranes. At a variety of different wavenumbers, the instrument measured the sorption of infrared irradiation. The wavenumber range that was used for the IR spectral measurement was from 400 cm^{-1} to 4000 cm^{-1}.

Porosity, Pore Size, and Water Uptake Analyses

Gravimetric method was adopted to assess the porosity characteristic of the membranes. A damp membrane sample of a particular dimension was given a weight. The sample was then dried until it achieved a constant weight in an oven at a temperature of 60 °C. Following that, the data was entered into Eq. (1). The water uptake analysis was done by immersing a dry membrane sample into water and comparing the weight of a wet and a dry condition. It was calculated using Eq. (2). The Guerout–Elford–Ferry Equation was utilized in order to get a rough approximation of the pore size in the membrane, as shown in Eq. (3), which considered the water permeability and physical properties.

$$\varepsilon = \frac{W_{1-}W_2}{\rho.\mathrm{A.l}}.100\% \quad (1)$$

$$wu = \frac{W_{1-}W_2}{W_2}.100\% \quad (2)$$

$$r_m = \sqrt{\frac{(2.9-1.75\varepsilon)8\eta.I.Q}{\varepsilon.A.\Delta P}} \quad (3)$$

Pure Water Flux (PWF)

The filtration test was conducted using a crossflow filtration cell, which allowed to mount a membrane sheet of 9.6 cm^2. The filtration was derived by transmembrane pressure of 1 bar with volumetric feed velocity of 60 ml min^{-1} at room temperature of 25 °C. At a rotation speed of 25 revolutions per minute, a peristaltic pump (manufactured by Watson Marlow in the United Kingdom) was used to circulate the supply water. Prior to the acquisition of filtration data, the membrane sample was compressed at a pressure of 1 bar until the water flux remained stable. The permeate collection period was set for 60 min. The permeate was collected at an interval of 60 min during the filtration period, until the obtained volume was constant as a function of time. In order to get reliable data, the procedure was repeated thrice on different membranes. Calculating the pure water flux (PWF, L m^{-2} h^{-1}) was done using Eq. (4).

$$\mathrm{PWF} = \frac{\Delta V}{\Delta t . A . \Delta P} \quad (4)$$

Filtration Performance and Anti-Fouling Property

As a foulant sample, a solution of humic acid with a concentration of 50 mg L^{-1} was used to assess the filterability of the developed membranes. The protocol and experimental parameters for the filtration were the same as the PWF, except for the feed solution. At a wavelength of 280 nm, a UV-Vis Spectrophotometry (U-2000, Hitachi Co., Japan) measurement was utilized in order to determine the amount of humic acid present in both the feed solution and the permeate solution. After that, Eq. (5) was applied in order to compute the amount of humic acid that was rejected by the membrane.

The Flux Recovery Ratio (FRR, %) measurement was utilized in order to evaluate the anti-fouling capability of the membrane. Following the filtration of purified water to determine the PWP, the feed solution was switched to a humic acid solution with a concentration of 50 mg L^{-1} to undergo a filtration process for 1 h. Afterward, the membrane coupon was flipped (active side facing permeate) to allow back washing using a pure water feed at a pressure of 1 bar for 10 min. Subsequently, the membrane coupon was flipped back (active side facing the feed) again, followed by pure water filtration for 1 h to obtain the second PWP.

$$\mathrm{R} = \frac{C_{0.feed} - C_{0.permeate}}{C_{0.feed}} \, x100\ \% \quad (5)$$

$$\mathrm{FRR} = \left(\frac{J_w}{J_{wr}}\right) \mathrm{x}100\% \quad (6)$$

RESULTS AND DISCUSSION

Characteristic of the Chitosan from Golden Snail's Shells using FTIR

The FTIR characteristic of the extracted chitosan from Golden Snail's shells is presented in Fig. 2. The FTIR measurement was carried out in order to determine whether or not the modified membranes contain any of the functional groups of chitosan which can be used as an indication that the modification is successful or not. The overall peaks are identical with the spectra reported in earlier work (Varma and Vasudevan, 2020). Chitosan had FTIR peaks at wavenumbers of 3642 cm^{-1}, 3518 cm^{-1}, 2980 cm^{-1}, 2872 cm^{-1}, 2513 cm^{-1}, 2355 cm^{-1}, 2139 cm^{-1}, 1863 cm^{-1}, 1676 cm^{-1}, 1651 cm^{-1}, 1080 cm^{-1}, 1016 cm^{-1}

and 874 cm^{-1} correspond to O-H (in alcohol), N-H (in amine), N-H (secondary amine), N-H (primary amine), C-H (aliphatic), O=C=O (carbon dioxide), S-C=N (thiocyanate), C=O (amide), C-N (cyano), C=N (oxyma), C-O (primary alcohol), S=O (Sulfate), and β-1,4 glycosidic (Glucose) clusters, respectively. Those functional groups are the attributes of chitosan. The FTIR spectra of the extracted chitosan from Golden Snail's shells was in line with the one obtained from earlier reports (Muchtar et al. 2019, Ghaemi et al. 2018). Those functional groups could enhance the polarity of the membrane when the chitosan remained in the polymer matrix and hence induce hydrophilic properties.

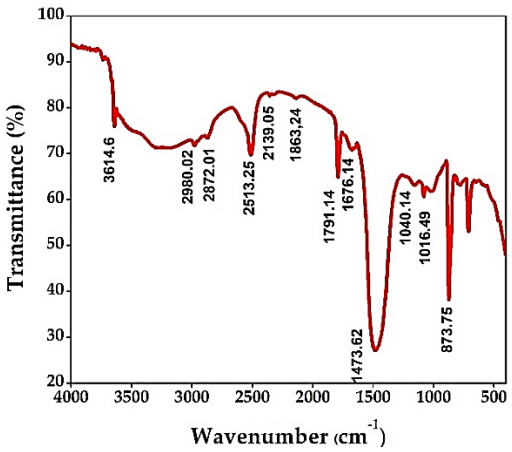

Fig. 2: FTIR of the chitosan isolated from golden snail shell.

Membrane Characteristics

Membrane Surface Hydrophilicity

Fig. 3 clearly shows the positive impact of chitosan in lowering the membrane surface contact angle. A low WCA value depicts the likelihood of a surface to be wetted by the membrane surface (Foong et al. 2020, Rekik et al. 2019). A membrane with a low WCA indicates that it is easily wetted by water (Geng et al. 2017). A hydrophilic surface typically poses a contact angle <90°. Hence, lower WCA is attributed to hydrophilic membrane, and vice versa (Al-Mubaddel et al. 2020). As shown in Fig. 3, all prepared membranes were hydrophilic, but the one loaded with, and higher loadings of chitosan showed a greater hydrophilicity.

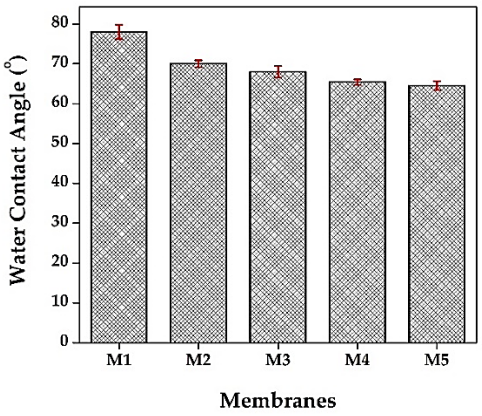

Fig. 3: Water contact angle of the PES membranes without and with the addition of chitosan extracted from golden snail shell in different loadings

The neat PES membrane (M1) was shown to offer the highest WCA, with a value of 78° ±1.8, as shown in Fig. 3. The high WCA can be attributed to the pristine PES property, a hydrophobic polymer (Kouhestani et al. 2019). The WCA of M2 increased to 70°±0.86 after the addition of a chitosan additive at a weight percent of 1% in the dope solution via blending, and further decreased to 68°±1.45 and 65,4°±0.70 with chitosan loadings of 3 wt%, 5 wt%, and 7 wt%. The increase in chitosan-loaded PES-based membrane hydrophilicity is thought to be caused by the abundance of hydroxyl groups on the chitosan (Ayodele et al. 2018). The hydroxyl group helps to facilitate the interaction between the water molecule and the membrane surface which is desirable in enhancing water permeability, and a lower likelihood of membrane fouling as discussed later. The existence of polar groups on the

surface of the membrane would make sites available for the formation of hydrogen bonds between the water molecule and the polymer matrix on the membrane surface (Muchtar et al. 2019).

Morphology

Fig. 4 displays images from a scanning electron microscope, which demonstrate the surface morphologies of all the prepared membranes. After chitosan was added to the dope solution, there was a discernible change in the surface morphology, as shown in the pictures. The virgin PES membrane (M1) had a perfectly smooth surface that was covered in holes that were evenly distributed across the entire surface. Loading chitosan as dope solution additive altered the surface morphology in terms of the quantity of surface pores and the size of those pores. Compared with M1, the pore mouths of M2, M3, M4 and M5 were larger. Because of the high concentration of hydrophilic groups, such changes in morphologies were caused by faster intrusion of nonsolvent into the cast film, which resulted in bigger pore sizes (Chrzanowska et al. 2018).

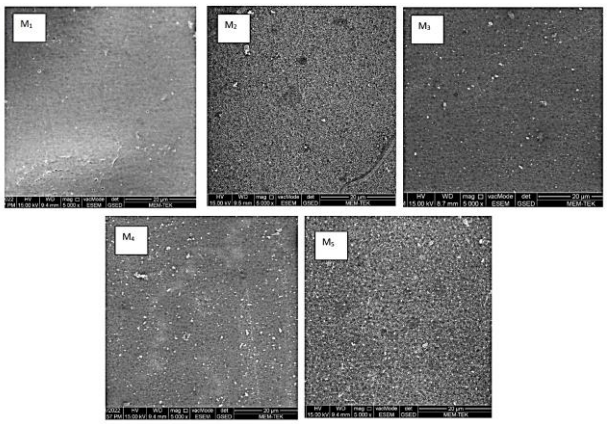

Fig. 4: SEM images of the PES membranes without and with the addition of chitosan extracted from golden snail shell in different loadings.

FTIR Spectra

Fig. 5 depicts the impact that chitosan loading has on the FTIR spectra of each of the produced membranes. It shows that the pristine PES membrane consisted of aromatic ring depicted by peaks at wavenumbers of 1450-1510 cm^{-1}, ether aromatic groups denoted by peaks at wavenumbers of 1230 cm^{-1} – 1270 cm^{-1}, sulfone group at 1100 cm^{-1} – 1200 cm^{-1}, and C-H in the aromatic ring at 670-900 cm^{-1} (Fathanah et al. 2020). The ring of the aromatic group (C=C-C) is depicted by peaks at wave numbers of 1483 cm^{-1}, ether aromatic (C-O-C) at 1249 cm^{-1}, sulfone group (O=S=O) at 1150 cm^{-1}, and C-H aromatic at 712 cm^{-1}. A new peak appeared at wavelength of 3440 cm^{-1} for the chitosan-loaded PES-based membrane assigned for OH from alcoholic and phenolic moieties in chitosan (Ayodele et al. 2018). The appearance of this peak suggested the effective modification of chitosan on the PES-based membrane.

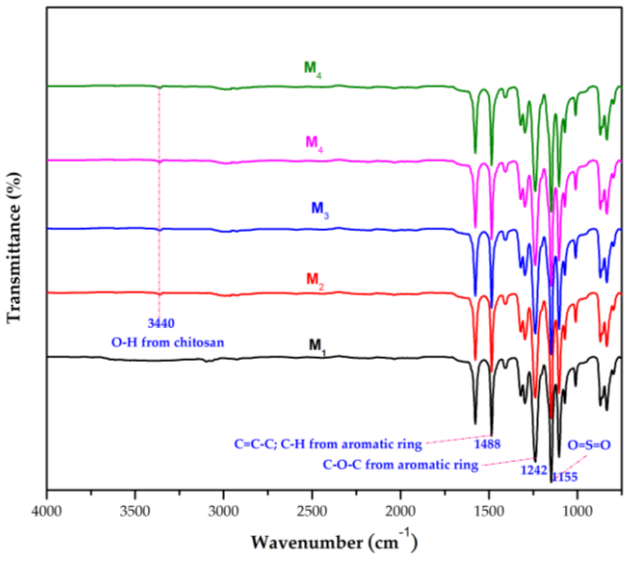

Fig. 5: FTIR spectrum of the PES membranes without and with the addition of chitosan extracted from golden snail shell in different loadings.

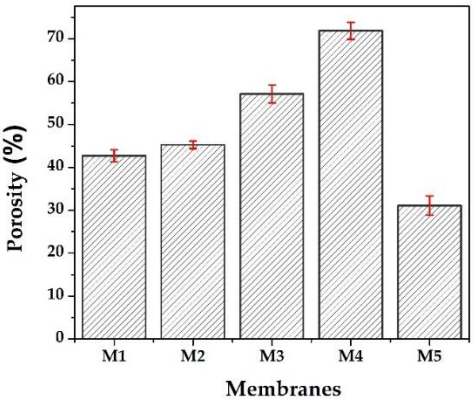

Fig. 6: Porosity of the PES membranes without and with the addition of chitosan extracted from golden snail shell in different loadings.

Porosity

The effects of chitosan loading on PES-based membrane porosity is presented in Fig. 6. In this bar chart, it is shown that chitosan loading led to higher porosity up to 5 wt% loading and drop to even below the pristine membrane for the 7wt% loading. Porosity reflects the fraction of void in the membrane matrix. The PES-based membrane that contained 5 weight percent of chitosan yielded the best results in terms of porosity (71.83%). The lowest porosity was obtained for M5 membrane. Membrane porosity is highly affected by the de-mixing process, and how the cast film behaves during the phase inversion. For cast film that contained hydrophilic substrate (i.e., chitosan), it has a higher affinity to water than the neat polymer. The transport of water (as nonsolvent) into the cast film was faster, leading to a higher volume of polymer lean phase during the phase inversion. The high fraction of the polymer lean phase eventually formed voids in the final membrane. It explains the increase in the porosity of M2, M3 and M4 compared to M1. Other than increasing the water affinity, the overloading of chitosan also increased the film viscosity, which hindered the water penetration into the cast film. It results in the formation of membrane matrix with a low porosity as shown for M5.

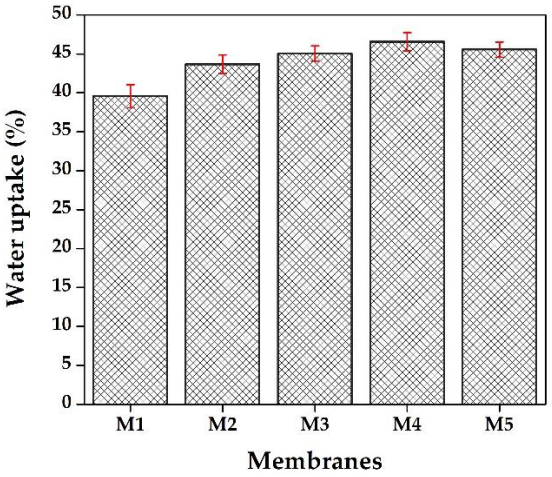

Fig. 7: Water uptake of the PES membranes without and with the addition of chitosan extracted from golden snail shell in different loadings

Water Uptake

Fig. 7 depicts the water uptake property of the prepared membrane showing an increasing value as a function of chitosan loading in the dope solutions. The water uptake parameter quantifies the water absorption into the membrane matrix. Membranes with hydrophilic property and high porosity would pose a high water uptake value, as shown by the trend in Fig. 7. It is shown that there was an increasing trend in water uptake in the following order M1 < M2 < M3 < M4 > M5 with the water uptake values of 39.56%, 43.67%, 45.05%, 46.56%, and 45.56%, respectively. They generally follow the porosity trend shown in Fig. 7, because the water up taken by the membrane could occupy the voids inside the membrane matrix. However, the water uptake of M5 did not fall under M1, like for the porosity. It can

be attributed to the hydrophilicity of M5, which was the highest among all prepared membranes (Fig. 3).

Pore Size

The estimated pore size of the prepared membranes obtained from the PWF, and the membrane properties is presented in Fig. 8. It shows that increasing the chitosan loadings led to larger membrane pore size up to 5 wt% in the dope solution. The estimated pore sizes of M1, M2, M3, M4 and M5 were 0.36 µm, 0.0587 µm, 0.0878 µm, 0.104 µm, and 0.0499 µm. M1 pores were smaller in size than M5 pores because M1 did not contain chitosan, which aids in pore formation and enlargement during the inversion phase. However, the porosity of this M1 membrane was quite high because the original PES membrane has a porous surface, due to the pores were very small or close to dense. M5 has lower porosity due to the excessive quantity of chitosan added, which clogs the membrane's surface, though it did aid in the creation of some larger size pores. This result is in agreement with previous work reported by Fathanah et al. (2022).

The trend is quite similar to the porosity and the water uptake. The size of the membrane pore is dictated by the thermodynamic and kinetic during the phase inversion. Up to 5 wt% loading of chitosan in the membrane matrix, it fastened the demixing, resulting in larger membrane pore size. Beyond that value (at 7 wt%), overloading of chitosan also increased the cast film viscosity, lowering the demixing rate, hence the resulting membrane pore size. Loading of chitosan increased the water affinity to the cast film, promoting a higher rate of solvent/nonsolvent exchange favorable for higher membrane pore size.

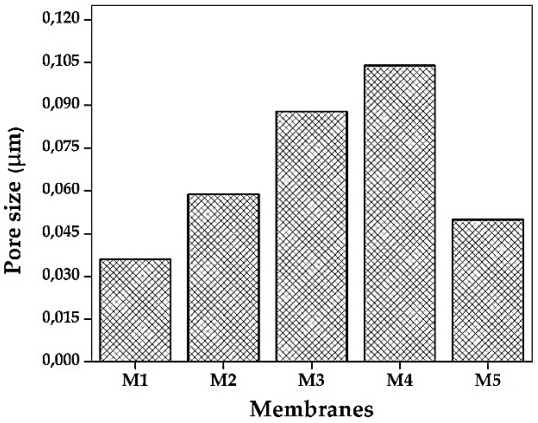

Fig. 8: Pore Size of the PES membranes without and with the addition of chitosan extracted from golden snail shell in different loadings

Pure Water Flux

Fig. 9 shows the PWF of all prepared membranes depicting the increasing trend up to M4, followed by a slight drop for M5. The pristine PES membrane had a PWF of 111 L m^{-2} h^{-1}. The PWF values increased to 125 L m^{-2} h^{-1}, 161 L m^{-2} h^{-1}, peaked at 181 L m^{-2} h^{-1}, and slightly decreased to 146 L m^{-2} h^{-1} for M2, M3, M4, and M5, with corresponding chitosan loadings of 1 wt%, 3 wt%, 5 wt%, and 7 wt%, respectively. The trend of the CWF can be well explained by the chemical and physical properties of the prepared membranes detailed earlier. High hydrophilicity, porosity, pore size, and water uptake favor a high PWF (Sri Abirami Saraswathi et al. 2017). This finding suggests that incorporating additives could effectively improve intrinsic membrane properties. Membranes with high PWF can help in lowering the footprint. Lesser membrane area is required to treat the same feed volume, leading to a lower energy footprint (pumping energy) and membrane investment (less membrane area). However, the extent of advantage offered by the membrane for a surface water treatment needs to be assessed when treating the feed.

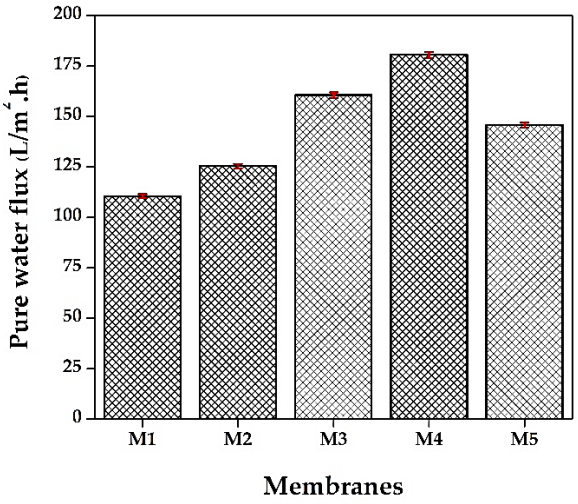

Fig. 9: Pure water flux of the PES membranes without and with the addition of chitosan extracted from golden snail shell in different loadings

Filtration Performance and Anti-Fouling Property

Flux and Rejection of Humic Acid Solution

The flux and the rejection of all prepared membranes when treating 50 mg L^{-1} of humic acid solution are presented in Fig. 10. The capability to retain humic acid under high flux over prolonged filtration duration is the true measure of membrane performance. The water flux trend resembles the PWP trend. The flux values increased from 70 L m^{-2} h^{-1} for M1, to 82 L m^{-2} h^{-1} and 95 L m^{-2} h^{-1}, respectively for M2 and M3, peaked at 120 for M4, then dropped to 78 L m^{-2} h^{-1} for M5. The humic acid solution flux trend can be explained similarly to the PWF.

As expected, an opposite trend was observed for humic acid rejection. It decreased from 92% for M1 to 75% for M2, 59% for M3 and reached the lowest value at 40% for M4, before increasing back to 66% for M5. If observed between M1 and M5, the gap in rejection is notable even though their pore properties were not significantly different. This is assumed because M1 has a denser surface with a high number of pores, but those pores are of a smaller size. In contrast, M5 has a small number of pores, but the size of those several pores is larger. As a result, the quantity of humic acid that could be retained on the surface is lower. This could be the reason to the fact that % Rejection of M1 was significantly higher than that of M5. In addition to this. The degree to which the membrane was hydrophilic was an important factor in the process. M1 has a higher WCA, which means it is hydrophobic, and this gives it a superior interaction when bonding humic acid particles to the surface.

The opposite trend of flux and rejection is common, considering the roles of pore size in promoting water permeation. A high pore size results in higher water permeation but lower particle retention (i.e., humic acid) (Muchtar et al. 2019). Humic acid that formed small clusters could pass through the membrane pores leading to a low rejection.

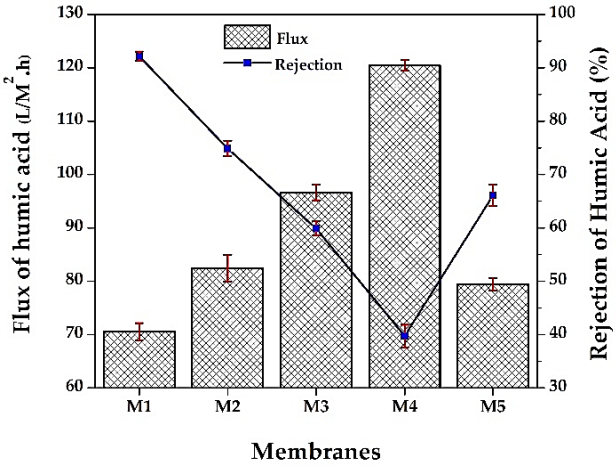

Fig. 10: The initial flux and the rejection of humic acid solution (50 mg L^{-1})

Anti-Fouling Property

Anti-fouling attribute is another critical parameter in judging a membrane performance, evaluated using FRR parameter. FRR indicates the capacity of the membrane

to restore its performance through physical cleaning (i.e., backwashing) after suffering from fouling. FRR also indicates the easiness of a membrane to undergo cleaning. Fig. 11 shows that the pristine PES had the lowest FRR value among all prepared membranes, attributed to its lowest hydrophilicity compared to the rest. This finding is consistent with an earlier work (Liu et al. 2020). The FRR values increased from M1 to M2, M3 and M4, then drop again for M5. Despite of having the lowest WCA, M5 still posed lower FRR than M2, M3 and M4. Available data in this study could not explain the quaint finding on the FRR of M5. Detailed analyses are still required to explain its relatively lower FRR despite of having the lowest WCA, and relatively lower pore size than M4.

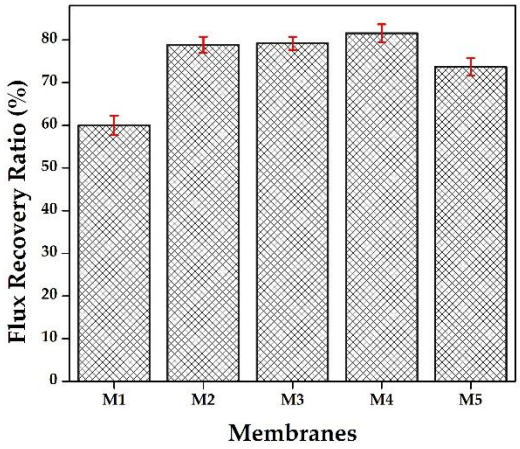

Fig. 11: Flux recovery ratio (FRR) of the PES membranes without and with the addition of chitosan extracted from golden snail shell in different loadings

Overall findings demonstrated a clear trend of chitosan in altering the resulting membrane properties and humic acid solution performance. In practice, an ideal membrane should pose both a high PWF and a high humic acid rejection. However, none of the prepared membranes achieved such objectives. In this case, further optimization should be conducted. The membrane performance must achieve a minimum threshold of humic acid rejection while maximizing the PWF. The threshold is typically defined on a case-by-case basis.

CONCLUSIONS

This study demonstrated that improved PES-based membrane performance in terms of water flux and FRR was effectively obtained by loading chitosan extracted from Golden Snail's shells. Loading of 5wt% chitosan in the dope solution (M4) resulted in the highest PWF and FRR of 181 (M1) L m^{-2} $h^{-1}$and 80%, respectively. Those values were far greater than the pristine PSF with the corresponding PWF and FRR of 111 L m^{-2} $h^{-1}$and 60%. The trend of PWF and humic acid solution flux were similar, in which the values increased from M1 to M4, and slightly dropped in M5. The trends were consistent and could be explained with the chemical and physical characteristics of the prepared membranes. The membranes loaded with chitosan had better hydrophilicity as shown by the lower contact angle. M4 showed the best performance for humic acid solution filtration thanks to its largest pore combined with good hydrophilicity. Overall results suggest a sensitive impact of a chitosan additive in dictating the resulting membrane properties and filtration performance. Using additives extracted from farming waste could contribute to the upcycling options of Golden Snail shells and increase the competitiveness of the farming industry.

ACKNOWLEDGEMENT

The authors wish to thank Universitas Syiah Kuala, Indonesia, for financial support granted through the Penelitian Profesor, Contract Number 145/UN11/SPK/PNBP/2022

NOMENCLATURE

w_1	:	the weight of the dried membrane sample
w_2	:	the weight of a wet membrane (g)
l	:	membrane thickness (m)
A	:	membrane surface area (m^2)
ρ	:	water density (0.998 g cm^{-1})
η	:	water viscosity (8.9 ×10-4 Pa s)
$\overline{\Delta P}$	:	operational pressure (MPa)
Q	:	the volumetric rate of water permeation (m^3 s^{-1})
ΔV	:	the permeate volume (L)
Δt	:	the filtration time (h)
C_f	:	the humic acid concentration in the feed solution (50 mg L^{-1})
C_p	:	the humic acid concentration in the permeate solution (mg L^{-1})
J_w	:	the initial PWF (L m^{-2} h^{-1}) before humic acid filtration
J_{wr}		the PWP after backwashing (L m^{-2} h^{-1})

REFERENCES

Ali, I., 2012. "New generation adsorbents for water treatment." *Chemical Reviews 112*, 5073–5091.

Al-Mubaddel, F.S., AlRomaih, H.S., Karim, M.R., Luqman, M., Al-Rashed, M.M., and Al-Mutairi, A.S., 2020. "Improved salt rejection, hydrophilicity and mechanical properties of novel thermoplastic polymer/chitosan nanofibre membranes." *Journal of Engineered Fibers and Fabrics*,*15*.

Ayodele, O., Okoronkwo, A.E., Oluwasina, O.O., and Abe, T.O., 2018. "Utilization of blue crab shells for the synthesis of chitosan nanoparticles and their characterization." *Songklanakarin Journal of Science and Technology, 40*, 1039–1042.

Chrzanowska, E., Gierszewska, M., Kujawa, J., Raszkowska-Kaczor, A., and Kujawski, W., 2018. "Development and characterization of polyamide-supported chitosan nanocomposite membranes for hydrophilic pervaporation." *Polymers, 10*, 1–21.

Elizalde, C.N.B., Al-Gharabli, S., Kujawa, J., Mavukkandy, M., Hasan, S.W., and Arafat, H.A., 2018. "Fabrication of blend polyvinylidene fluoride/chitosan membranes for enhanced flux and fouling resistance." *Separation and Purification Technology, 190*, 68–76.

Fathanah, U., Machdar, I., Riza, M., Arahman, N., Wahab, M.Y., Muchtar, S., Rosnelly, C.M., Mulyati, S., Syamsuddin, Y., Juned, S., and Razi, F., 2022. "Effect of hybrid $Mg(OH)_2$/chitosan on the hydrophilicity and antifouling of polyethersulfone (PES) membrane." *Rasayan Journal of Chemistry, 15*, 813–823.

Fathanah, U., Machdar, I., Riza, M., Arahman, N., Yusuf, M., Muchtar, S., Bilad, M.R., and Nordin, N.A.H., 2020. "Enhancement of antifouling of ultrafiltration polyethersulfone membrane with hybrid Mg $(OH)_2$/chitosan by polymer blending." *Journal of Membrane Science and Research, 6*, 375–382.

Foong, Y.X., Yew, L.H., and Chai, P. V., 2020. "Green approaches to polysulfone based membrane preparation via dimethyl sulfoxide and eco-friendly natural additive gum Arabic." *Materials Today: Proceedings, 46*, 2092–2097.

Gao, K., Li, T., Liu, J., Dong, B., and Chu, H., 2019. "Ultrafiltration membrane fouling performance by mixtures with micromolecular and macromolecular organics." *Environmental Science: Water Research and Technology, 5*, 277–286.

Geng, Z., Yang, Xue, Boo, C., Zhu, S., Lu, Y., Fan, W., Huo, M., Elimelech, M., and Yang, Xia, 2017. "Self-cleaning anti-fouling hybrid ultrafiltration membranes via side chain grafting of poly(aryl ether sulfone) and titanium dioxide." *Journal of Membrane Science, 529*, 1–10.

Ghaemi, N., Daraei, P., and Akhlaghi, F.S., 2018. "Polyethersulfone nanofiltration membrane embedded by chitosan nanoparticles: Fabrication, characterization and performance in nitrate removal from water." *Carbohydrate Polymers ,191*, 142–151.

Guan, Y.F., Qian, C., Chen, W., Huang, B.C., Wang, Y.J., and Yu, H.Q., 2018. "Interaction between humic acid and protein in membrane fouling process: A spectroscopic insight." *Water Research ,145*, 146–152.

Hariani, P.L., Riyanti, F., Fatma, Rachmat, A., and Herbanu, A., 2020. "Removal of Pb(II) using hydroxyapatite from golden snail shell (*Pomacea canaliculata l.*) modified with silica." *Molekul, 15*, 130–139.

Idris, A., Mat Zain, N., and Noordin, M.Y., 2007. "Synthesis, characterization and performance of asymmetric polyethersulfone (PES) ultrafiltration membranes with polyethylene glycol of different molecular weights as additives." *Desalination 207*, 324–339.

Jubaedah, D., Wijayanti, M., Marsi, M., and Rizaldy, N., 2018. "Utilization of Golden Apple Snail (Pomacea canaliculata) S hells as Liming Materials for Pangasius sp Culture in Swamp Fish Pond." *E3S Web of Conferences, 68*, 2–7.

Kouhestani, F., Torangi, M.A., Motavalizadehkakhky, A., Karazhyan, R., and Zhiani, R., 2019. "Enhancement strategy of polyethersulfone (PES) membrane by introducing pluronic F127/graphene oxide and phytic acid/graphene oxide blended additives: Preparation, characterization and wastewater filtration assessment." *Desalination and Water Treatment, 171*, 44–56.

Kumar, R., Isloor, A.M., Ismail, A.F., and Matsuura, T., 2013. "Synthesis and characterization of novel water soluble derivative of chitosan as an additive for polysulfone ultrafiltration membrane." *Journal of Membrane Science, 440*, 140–147.

Liu, J., Tian, C., Xiong, J., and Wang, L., 2017. "Polypyrrole blending modification for PVDF conductive membrane preparing and fouling mitigation." *Journal of Colloid and Interface Science, 494*, 124–129.

Liu, R., Liu, S., Yu, J., Zhang, W., Dai, J., Zhang, Y., and Zhang, G., 2020. "The construction of a hydrophilic inorganic layer enables mechanochemically robust super antifouling UHMWPE composite membrane surfaces." *Polymers, 12*, 1–17.

Miller, D.J., Paul, D.R., and Freeman, B.D., 2014. "An improved method for surface modification of porous water purification membranes." *Polymer, 55*, 1375–1383.

Muchtar, S., Wahab, M.Y., Mulyati, S., Arahman, N., and Riza, M., 2019a. "Superior fouling resistant PVDF membrane with enhanced filtration performance fabricated by combined

blending and the self-polymerization approach of dopamine." *Journal of Water Process Engineering, 28*, 293–299.

Nasrollahi, N., Vatanpour, V., Aber, S., and Mohammad, N., 2018. "Preparation and characterization of a novel polyethersulfone (PES) ultra filtration membrane modified with a CuO / ZnO nanocomposite to improve permeability and antifouling properties." *Separation and Purification Technology, 192*, 369–382.

Nayab, S.S., Abbas, M.A., Mushtaq, S., Niazi, B.K., Batool, M., Shehnaz, G., Ahmad, N., and Ahmad, N.M., 2021. "Anti-foulant ultrafiltration polymer composite membranes incorporated with composite activated carbon/chitosan and activated carbon/thiolated chitosan with enhanced hydrophilicity." *Membranes, 11*, 827.

Ouda, M., Hai, A., Krishnamoorthy, R., Govindan, B., Othman, I., Kui, C.C., Choi, M.Y., Hasan, S.W., and Banat, F., 2022. "Surface tuned polyethersulfone membrane using an iron oxide functionalized halloysite nanocomposite for enhanced humic acid removal." *Environmental Research, 204*, 112113.

Phewphong, S., Roschat, W., Pholsupho, P., Moonsin, P., Promarak, V., and Yoosuk, B., 2022. "Biodiesel production process catalyzed by acid-treated golden apple snail shells (Pomacea canaliculata)-derived CaO as a high-performance and green catalyst." *Engineering and Applied Science Research, 49*, 36–46.

Rahmi, Julinawati, Nina, M., Fathana, H., and Iqhrammullah, M., 2022. "Preparation and characterization of new magnetic chitosan-glycine-PEGDE (Fe_3O_4/Ch-G-P) beads for aqueous Cd(II) removal." *Journal of Water Process Engineering, 45*, 102493.

Rambabu, K., Bharath, G., Monash, P., Velu, S., Banat, F., Naushad, M., Arthanareeswaran, G., and Loke Show, P., 2019. "Effective treatment of dye polluted wastewater using nanoporous $CaCl_2$ modified polyethersulfone membrane." *Process Safety and Environmental Protection, 124*, 266–278.

Rekik, S.B., Gassara, S., Bouaziz, J., Deratani, A., and Baklouti, S., 2019. "Enhancing hydrophilicity and permeation flux of chitosan/kaolin composite membranes by using polyethylene glycol as porogen." *Applied Clay Science, 168*, 312–323.

Shen, J. nan, Ruan, H. min, Wu, L. Guang, and Gao, C. Jie, 2011. "Preparation and characterization of PES-SiO_2 organic-inorganic composite ultrafiltration membrane for raw water pretreatment." *Chemical Engineering Journal, 168*, 1272–1278.

Sri Abirami Saraswathi, M., Kausalya, R., Kaleekkal, N.J., Rana, D., and Nagendran, A., 2017. "BSA and humic acid separation from aqueous stream using polydopamine coated PVDF ultrafiltration membranes." *Journal of Environmental Chemical Engineering, 5*, 2937–2943.

Susanto, H., Robbani, M.H., Istirokhatun, T., Firmansyah, A.A., and Rhamadhan, R.N., 2020. "Preparation of low-fouling polyethersulfone ultrafiltration membranes by incorporating high-molecular-weight chitosan with the help of a surfactant." *South African Journal of Chemical Engineering, 33*, 133–140.

Varma, R., and Vasudevan, S., 2020. "Extraction, characterization, and antimicrobial activity of chitosan from

horse mussel modiolus modiolus." *ACS Omega, 5*, 20224–20230.

Vatsha, B., Ngila, J.C., and Moutloali, R.M., 2014. "Preparation of antifouling polyvinylpyrrolidone (PVP 40K) modified polyethersulfone (PES) ultrafiltration (UF) membrane for water purification." *Physics and Chemistry of the Earth, 67–69*, 125–131.

Wang, T. xu, Chen, S. ruo, Wang, T., Wu, L. guang, and Wang, Y. Xing, 2022. "PES mixed-matrix ultrafiltration membranes incorporating ZIF-8 and poly(ionic liquid) by microemulsion synthetic with flux and antifouling properties." *Applied Surface Science, 576*, 151815.

Yuan, S., Li, Jian, Zhu, J., Volodine, A., Li, Jiansheng, Zhang, G., Van Puyvelde, P., and Van der Bruggen, B., 2018. "Hydrophilic nanofiltration membranes with reduced humic acid fouling fabricated from copolymers designed by introducing carboxyl groups in the pendant benzene ring." *Journal of Membrane Science, 563*, 655–663.

Zhao, S., Tao, Z., Chen, L., Han, M., Zhao, B., Tian, X., Wang, L., and Meng, F., 2021. "An antifouling catechol/chitosan-modified polyvinylidene fluoride membrane for sustainable oil-in-water emulsions separation." *Frontiers of Environmental Science and Engineering, 15*, 63.

Zhu, R., Diaz, A.J., Shen, Y., Qi, F., Chang, X., Durkin, D.P., Sun, Y., Solares, S.D., and Shuai, D., 2018. "Mechanism of humic acid fouling in a photocatalytic membrane system." *Journal of Membrane Science, 563*, 531–540.